Modelling of Fixed Speed Squirrel Cage Induction Generators for Small Signal Stability Assessment

BHINAL MEHTA[1], PRAGHNESH BHATT[1], VIVEK PANDYA[2]
[1]Department of Electrical Engineering, C.S. Patel Institute of Technology, CHARUSAT, Changa, Gujarat, INDIA
[2] Department of Electrical Engineering, School of Technology, PDPU, Gandhinagar, Gujarat, INDIA
Corresponding Author: BHINAL MEHTA, email: bhinalmehta.ee@charusat.ac.in,
Mobile: +919427045058

Abstract—Fixed speed squirrel cage induction generators (FSIG) for the wind power generations have been widely used worldwide due to its salient features like cost effectiveness, simplicity and robustness. It takes utmost importance to analyse their impact on power system stability as their penetration levels are continuously increasing. The state space approach is presented to analyse both small signal and transient stability by developing a mathematical model of full order squirrel cage induction generator. The small signal behaviour of FSIG has been studied for both one-mass and two-mass model representation of drive train. The eigenvalue and participation factor analysis for developed state space model of FSIG connected to infinite bus are carried out to identify the nature of modes of oscillations under different operating conditions such as varying wind speed and grid strength. The transient analyses are also presented to investigate the capability of FSIG to satisfy the Grid Code requirements.

Key-words— Fixed Speed Induction Generator, Drive Train, Eigenvalue Analysis, Small Signal Stability, Fault Ride Through

1 Introduction

The use of wind power has increased significantly over recent decades and its integration with the power system is now an important topic of study. India ranks fifth amongst the wind-energy-producing countries of the world after USA, China, Germany and Spain. The installed capacity of wind power in India has reached about 20 GW by 2013 [1]. The small signal behaviour of power systems has been dominated by the electromechanical interactions between the synchronous generators through the transmission network for conventional power system. Similarly, it is also important to assess the impact of wind turbine generating units on the system stability and vice versa as their penetration is continuously increasing [2]-[4].

The wind farms are generally located far from demand centres where the network is relatively weak and congested. Therefore, if the integration and penetration of wind energy are not properly assessed for the given network, it is difficult to maintain the reliability and stability [5]. In order to protect the security and operation of the transmission system, it is imperative to investigate the impact of wind at various penetration levels [6]. A detailed investigation into the inherent characteristics of squirrel-cage induction generator, doubly fed induction generator (DFIG) and permanent-magnet synchronous generator-based wind turbines using small-signal analyses to see how each turbine technology affects the local, inter-area, torsional and control modes of the system is carried out in [7].

Various comprehensive studies regarding the modelling of FSIG and DFIG and to identify their interaction with the power system have been reported in [8]-[14]. The impacts of wind generation are assessed and compared between FSIG and DFIG in [8],[9],[18] with regard to power system disturbances and change in network frequency. The modelling and performance effects of induction generator-based wind farms on the oscillation stability of power systems for multi-machine systems is discussed in [10]. The dynamic behaviour of FSIG wind turbines under wind speed fluctuations and system disturbances is investigated in [11],[12] where the identification of the nature of transient instability and system variables involved in the instability is carried out.

Most of the countries have their own grid codes to integrate WTGs into the utility grid. One of the primary grid code for WTGs is fault ride through also known as low voltage ride through (LVRT) capability. The regulations of grid integration are making these requirements mandatory for WTGs with high penetration level. [13]-[14],[19]

The mathematical modelling of full order FSIG for carrying out small signal after the grid integrations have not been reported in detail in

literature. Also, the effects of one-mass and two-mass model representation used for drive train in FSIG based wind turbine generators have not been compared from small signal stability viewpoint. Therefore, the objectives of the paper are as follows.

1. To formulate state space model of full order FSIG connected to infinite bus for small signal stability assessment.
2. To compare the small signal behaviour of FSIG connected to infinite bus with one mass and two mass drive train model.
3. To investigate the nature of modes of oscillations with varying wind conditions and with different strength of transmission network.
4. To quantify the impact of pitch controller on small signal behaviour of the test system.
5. To investigate the fault ride through capability of FSIG under fault and voltage sag conditions

The paper is organized in five sections. Section 2 presents the mathematical modelling concepts associated with FSIG. Interfacing of FSIG with infinite bus is discussed in section 3. Section 4 details the approach developed to analyse the impact of FSIG on small signal and transient stability along with results and discussions of different scenarios followed by the conclusion in section 5.

2 Mathematical Modelling of FSIG

The schematic of wind turbine generator employing squirrel cage induction machine is shown in Fig.1. The wind turbine generating system employs squirrel cage induction generator in which the stator windings are directly connected to the three phase grid and rotor windings are short circuited. The slip of the generator varies with the amount of power generated. However, these variations are very small (1–2%), hence referred as constant speed or fixed-speed wind turbine generator.

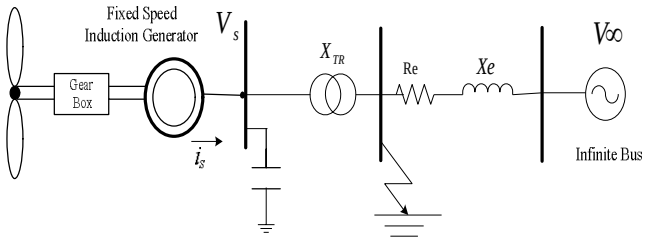

Fig.1.Schematic of a FSIG based wind turbine generator connected to an infinite bus

2.1 Induction Generator Model

Assumptions:

The following assumptions are made while modelling the induction generator.

(1) Stator current is negative when flowing toward the machine, i.e. generator convection is used
(2) Equations are derived in the synchronous reference frame
(3) q-axis is 90^0 ahead of the d-axis.

The stator of the induction machine carries three-phase windings. The windings produce a rotating magnetic field which rotates at synchronous speed. The dynamic equations for stator and rotor in d-q reference frame rotating at synchronous speed[15],[16],[18] are described in (1)-(3).

Stator Voltage Equations:

$$\begin{bmatrix} v_{ds} \\ v_{qs} \end{bmatrix} = R_s \begin{bmatrix} -i_{ds} \\ -i_{qs} \end{bmatrix} + \omega_s \begin{bmatrix} -\varphi_{qs} \\ \varphi_{ds} \end{bmatrix} + \frac{1}{\omega_b}\frac{d}{dt}\begin{bmatrix} \varphi_{ds} \\ \varphi_{qs} \end{bmatrix} \quad (1)$$

Rotor Voltage Equations:

$$\begin{bmatrix} v_{dr} \\ v_{qr} \end{bmatrix} = R_r \begin{bmatrix} i_{dr} \\ i_{qr} \end{bmatrix} + s\omega_s \begin{bmatrix} -\varphi_{qr} \\ \varphi_{dr} \end{bmatrix} + \frac{1}{\omega_b}\frac{d}{dt}\begin{bmatrix} \varphi_{dr} \\ \varphi_{qr} \end{bmatrix} \quad (2)$$

Flux Equations:

$$\begin{aligned} \varphi_{ds} &= -X_{ss} i_{ds} + X_m i_{dr} \\ \varphi_{qs} &= -X_{ss} i_{qs} + X_m i_{qr} \\ \varphi_{dr} &= X_{rr} i_{dr} - X_m i_{ds} \\ \varphi_{qr} &= X_{rr} i_{qr} - X_m i_{qs} \end{aligned} \quad (3)$$

where v_{ds} and v_{qs} are d- and q-axis stator voltages, respectively, v_{dr} and v_{qr} are d- and q-axis rotor voltages, respectively, i_{ds} and i_{qs} are d- and q-axis stator currents, respectively, i_{dr} and i_{qr} are d- and q-axis rotor currents respectively, R_s is stator resistance, R_r is rotor resistance, φ_{ds} and φ_{qs} are d- and q-axis stator fluxes, respectively, φ_{dr} and φ_{qr} are d- and q-axis rotor fluxes, respectively, ω_s is synchronous speed, ω_b is the base speed, X_{ss}, X_{rr}, and X_m stator reactance, rotor reactance and self magnetizing reactance, repectively.

The expression for the stator and rotor currents as the state variables are obtained by substituting the flux equations (3), into the stator and rotor voltage equations (1),(2).

2.2 Wind Turbine Model

To complete the induction generator state model, it is necessary to combine the equations that describe electrical voltage and current components of the machine with swing equation that provides rotor speed as state variable. In power system studies, drive trains are modelled as a series of rigid disks connected via mass less shafts.

2.2.1 One Mass Model of Drive Train

For small signal stability analysis of synchronous generators in conventional power plants, the one

mass or lumped mass model is used because the drive train behaves as a single equivalent mass. The participations of all inertias, which include the rotating masses of turbine and generator rotor, are nearly equal. Hence the mode of interest is non-torsional [15]. Similarly in case of wind turbine generating systems, drive train can be represented by the lumped mass system, where there is only a single inertia which is equivalent to the sum of the generator rotor and the wind turbine. The mathematical equation of a one-mass model is given by (4).

$$\frac{d\omega_r}{dt} = \frac{1}{2H_{tot}}(T_m - T_e) \quad (4)$$

where, H_{tot} is the total inertia of generator rotor and wind turbine, ω_r= generator rotor angle speed, T_m = mechanical torque torque and T_e = electromagnetic torque.

2.2.2 Two Mass Model of Drive Train

For accurate representation of drive train, wind turbine shaft and generator rotor coupled together via gear box which cannot be considered stiff. Therefore, the interaction between the wind turbine and generator rotor makes the shaft motion more complex than one mass model. The dynamics of the drive train which actually comprises of turbine, gearbox, shafts and other mechanical components of WT can be represented as two mass model i.e one mass for the wind turbine and the other for the generator rotor. The dynamic equations which represent two mass model of drive train obtained from Newton's equations of motion for rotational speed and shaft torsion are expressed in (5)-(8).

$$\frac{d\omega_t}{dt} = \frac{1}{2H_t}(T_m - T_{sh}) \quad (5)$$

$$\frac{d\theta_{tw}}{dt} = \omega_b(\omega_t - \omega_r) \quad (6)$$

$$T_{sh} = K_{sh}\theta_{tw} + D_{sh}\frac{d\theta_{tw}}{dt} \quad (7)$$

$$\frac{d\omega_r}{dt} = \frac{1}{2H_g}(T_m - T_e) \quad (8)$$

where H_t = inertia constant of turbine, H_g = inertia constant of generator, ω_t = WT angle speed, θ_{tw} = shaft twist angle, K_{sh} = shaft stiffness coefficient, D_{sh} = damping coefficient, T_{sh} = shaft torque.
T_m and T_e are given by (9) and (14).

$$T_m = \frac{C_{p(pu)}V_{w(pu)}{}^3}{\omega_{r(pu)}} \quad (9)$$

$$V_{w(pu)} = \frac{V_w}{V_{w\_base}} \quad (10)$$

$$C_{p(pu)} = \frac{C_p}{C_{p\_nom}} \quad (11)$$

where

$$C_p = c_1\left(\frac{c_2}{\lambda_i} - c_3\beta - c_4\right)e^{-c_5\lambda_i + c_6\lambda} \quad (12)$$

$$\lambda_i = \frac{1}{\frac{1}{\lambda + 0.08\beta} - \frac{0.035}{\beta^3 + 1}} \quad (13)$$

where, ρ = air density, R= WT blade radius, V_w = wind speed, β =blade pitch angle, λ= blade tip speed ratio, C_p= power coefficient. T_e in terms of the state variables

$$T_e = X_m(i_{dr}i_{qs} - i_{qr}i_{ds}) \quad (14)$$

2.3 Pitch Controller

The pitch angle of the wind turbine blade is controlled to maintain the rotating speed of the WT to prevent overrated power production during strong wind conditions. Generally, the reference of the pitch angle β_{ref} is kept zero when wind speed is below rated value. When wind speed is higher than rated value, the power limitation feature is activated by adjusting the pitch angle using the pitch controller [17]. The control equation is given by (15)

$$\frac{d\beta}{dt} = K_p\frac{T_m - T_{sh}}{2H_t} + K_i\Delta\omega_t \quad (15)$$

where, K_p and K_i are the proportional and integrating gains of the WT speed regulator, respectively. $\Delta\omega_t$ is the deviation of the WT rotating speed.

3 Interfacing of FSIG with InfiniteBus

The test system for the analysis is shown in Fig. 1 where FSIG is integrated to the infinite bus through the transmission line. The infinite bus is considered as voltage source of constant voltage and constant frequency. To carry out the small signal stability analysis of the system shown in Fig.1, the linearization of the induction machine equations given in (1)-(2) and the rotor mechanical equation given in (4) are presented in (16) and (17).

$$\dot{x} = Ax + Bu \quad (16)$$

$$y = Cx + Du \quad (17)$$

where, $\dot{x} = [i_{ds}\ \ i_{qs}\ \ i_{dr}\ \ i_{qr}\ \omega_r\ ]^T$ (18)

As the rotor is short circuited in case of squirrel cage induction generator, v_{dr} and v_{qr} are considered to be zero.

$$v_{dr} = v_{qr} = 0 \quad (19)$$

In general, input and output vectors for the system under considerations are defined as follows

$$u = [v_{ds}\ \ v_{qs}]^T \quad (20)$$

$$y = [i_{dr}\ \ i_{qr}]^T \quad (21)$$

System matrix A, Control matrix B, Output matrix C and Feed forward matrix D are represented in Appendix III. In order to consider the effect of transmission network, the stator voltage equations are represented in (22)-(23).

$$v_{ds} = v_{d\infty} - X_T i_{qs} + R_T i_{ds} \quad (22)$$

$$v_{qs} = v_{d\infty} + X_T i_{ds} + R_T i_{qs} \quad (23)$$

where, $X_T = X_{TR} + X_e$ (24)

$$R_T = R_e + R_S \quad (25)$$

where $v_{q\infty}$ and $v_{d\infty}$ are q and d axis components of infinite bus voltage.

The system matrixA_{sys}, for FSIG shown in Fig. 1 with the grid integration is given in (26).

$$A_{sys} = \begin{bmatrix} A_{11} & A_{12} & A_{13} & A_{14} & A_{15} \\ A_{21} & A_{22} & A_{23} & A_{24} & A_{25} \\ A_{31} & A_{32} & A_{33} & A_{34} & A_{35} \\ A_{41} & A_{42} & A_{43} & A_{44} & A_{45} \\ A_{51} & A_{52} & A_{53} & A_{54} & A_{55} \end{bmatrix} \quad (26)$$

The elements of system matrix A_{sys} are represented in Appendix IV.

4 Results and Discussions

4.1 Test Scenario

The impacts of FSIG on dynamic behaviour of power system under different wind conditions and with two drive train models have been evaluated for the test system shown in Fig. 1. The performance of FSIG is also evaluated with and without pitch controller for different operating conditions. The test scenarios considered with full order model of FSIG for the simulations are described below.

Scenario1. One mass model of drive train with pitch angle control

Scenario2. Two mass model of drive train without pitch angle control

Scenario3. Two mass model of drive train with pitch angle control

It has been observed that the dynamic performance of the power system is also affected by the strength of the transmission network to which the wind farms are connected. Hence, strong and weak transmission network are considered with short circuit level of 60 MVA and 25 MVA, respectively. The above three scenario are simulated for the following two cases.

Case1: Strong connection with short circuit level of 60 MVA

Case2: Weak connection with short circuit level of 25 MVA.

4.2 Small Signal Stability Analysis

Modal analysis or small signal analysis has been popularly used in power system for identification of low frequency oscillation. Small signal stability studies are based on linearization of system equations around the operating point and modes of oscillations of system response can be derived from the eigenvalues of the system state matrix. The analysis of the eigen properties of system state matrix provides valuable information regarding the stability characteristics of the system [15].

The states associated in the eigenvalue analysis for above three scenarios are listed in Table 1. The dynamic performance of FSIG is evaluated under different operating conditions such as varying wind speed, varying network strength and considerations of the pitch angle controllers. The steady state initial operating points for these varying operating conditions are tabulated in Table 2-4.

The results of eigenvalue analysis including frequency of oscillation, damping ratio and percentage participation of all the states for three scenarios under considerations are tabulated in Tables 5-10. The results shown in the Tables 5-10 reveal that system exhibit the stable behaviour for all the scenarios with varying wind speeds.

For scenario 1, four stable modes have been identified for each wind speed, two of which are non oscillating modes. The physical nature of the modes can be identified by observing the participation factors: $\lambda_{1,2}$, and $\lambda_{3,4}$ are oscillating modes associated with the stator and the rotor electrical dynamics, respectively. λ_5 is non oscillating mode associated with rotor electrical and mechanical dynamics (rotor currents and generator speed). λ_6 is also non oscillating mode associated with pitch angle dynamics. The stator mode has a large real part magnitude and the much higher frequency of oscillations which results in lowest damping ratio.

For Scenario 2, again four stable modes have been identified for each wind speed, three of which are oscillating modes. The participation factor reveals that $\lambda_{1,2}$, are associated with the stator electrical dynamics. The consideration of the two mass model has introduced an electromechanical mode $\lambda_{3,4}$ which is associated with rotor speed and shaft dynamics. $\lambda_{,6,7}$ are also an oscillating mode associated with rotor electrical and mechanical dynamics (rotor currents and generator speed). λ_5 is a non oscillating mode associated with rotor electrical dynamics which exhibits oscillating nature for scenario 1. For a two mass model of drive train, mechanical state variables contribute to two modes. One is of low frequency with higher damping ratio (Table 8:f=1.55 Hz,ζ= 26.25% at V_w = 9m/s) and the other is of higher frequency with lower damping ratio (Table 8:f=10.54 Hz,ζ= 3.5% at V_w = 9m/s).

For Scenario 3, five stable modes have been identified for each wind speed, three of which are oscillating mode and two are non oscillating. The participation factor reveals that $\lambda_{1,2}$, are oscillating mode associated with the stator electrical dynamics. $\lambda_{3,4}$ and $\lambda_{5,6}$ are also oscillating mode associated with rotor speed and shaft dynamics and rotor electrical dynamics, respectively. λ_7 and λ_8 are non oscillating mode associated with rotor speed and shaft dynamics and pitch angle dynamics.

Table 1: Identification of States and Associated Mode Numbers

Cases	Name of associated states	Mode numbers of associated states	Total number of states
Case 1	ids, iqs , ωr, β, idr, iqr	$\lambda_1,\lambda_2,\lambda_3,\lambda_4,\lambda_5,\lambda_6$	6
Case 2	ids, iqs , ωr, idr, iqr, ωt,θtω	$\lambda_1,\lambda_2,\lambda_3,\lambda_4,\lambda_5,\lambda_6,\lambda_7$	7
Case 3	ids, iqs , ωr, β, idr, iqr, ωt,θtω	$\lambda_1,\lambda_2,\lambda_3,\lambda_4,\lambda_5,\lambda_6,\lambda_7,\lambda_8$	8

Table 2: Operating Points for Scenario 1 (Initial Values)

Wind Speed in m/s	Tm in pu	Case 1 Strong Connection Short Circuit Level 60 MVA						Case 2 Weak Connection Short Circuit Level 25 MVA					
		ids0	iqs0	ωr0	β0	idr0	iqr0	ids0	iqs0	ωr0	β0	idr0	iqr0
7	0.3243	-0.274	0.322	1.002	0	-0.033	0.337	-0.278	0.321	1.002	0	-0.039	0.34
9	0.896	-0.494	0.886	1.006	0	-0.261	0.927	-0.546	0.881	1.006	0	-0.321	0.932
11	0.9257	-0.494	0.886	1.006	8.679	-0.261	0.927	-0.546	0.881	1.006	8.684	-0.321	0.932

Table 3: Operating Points for Scenario 2 (Initial Values)

Wind Speed in m/s	Case 1 Strong Connection Short Circuit Level 60 MVA							Case 2 Weak Connection Short Circuit Level 25 MVA						
	ids0	iqs0	ωr0	idr0	iqr0	ωt0	θtω0	ids0	iqs0	ωr0	idr0	iqr0	ωt0	θtω0
7	-0.274	0.323	1.002	-0.033	0.338	1.002	0.032	-0.278	0.322	1.002	-0.04	0.341	1.002	0.032
9	-0.497	0.891	1.006	-0.264	0.932	1.006	0.09	-0.55	0.886	1.006	-0.325	0.938	1.006	0.09
10	-0.516	0.921	1.006	-0.284	0.963	1.006	0.093	-0.574	0.915	1.006	-0.35	0.968	1.006	0.093

Table 4: Operating Points for Scenario 3 (Initial Values)

Wind Speed in m/s	Case 1 Strong Connection Short Circuit Level 60 MVA								Case 2 Weak Connection Short Circuit Level 25 MVA							
	ids0	iqs0	ωr0	β0	idr0	iqr0	ωt0	θtω0	ids0	iqs0	ωr0	β0	idr0	iqr0	ωt0	θtω0
7	-0.274	0.322	1.002	0	-0.033	0.337	1.002	0.032	-0.278	0.321	1.002	0	-0.039	0.34	1.002	0.032
9	-0.494	0.886	1.006	0	-0.261	0.927	1.006	0.089	-0.546	0.881	1.006	0	-0.321	0.932	1.006	0.089
11	-0.494	0.886	1.006	8.679	-0.261	0.927	1.006	0.089	-0.546	0.881	1.006	8.684	-0.321	0.932	1.006	0.089

Table 5: Small Signal Stability Analysis of FSIG for Scenario 1 at Different Wind Speed

Case 1 Strong Connection Short Circuit Level 60 MVA			
Eigenvalues	**Frequency of Oscillation (in Hz)**	**Damping Ratio**	**Most influential state in the control of the Mode with their participation factor (in percentage)**
Wind Speed 7 m/s			
-16.33±451.91	71.92	0.0361	ids=25.8,iqs=25.8,idr=24.1,iqr=24.2
-4.04±21.03	3.34	0.1889	ids=17.8,iqs=30,idr=19.1,iqr=32.2
-4.72	0	1	ids=42.7,iqs=3,wr=4.8,idr=45.9,iqr=3.3
-1.00	0	1	ids=1.7,iqs=0.4,wr=0.25,beta=95.3,idr=1.8,iqr=0.5
Wind Speed 9 m/s			
-16.22±451.87	71.91	0.0358	ids=25.8,iqs=25.8,idr=24.1,iqr=24.2
-3.58±11.64	1.85	0.2946	ids=1.97,iqs=44.8,wr=3,idr=2.1,iqr=48
-5.84	0	1	ids=47.2,iqs=0.9,idr=50.6,iqr=1
-1.19	0	1	beta=99.9
Wind Speed 11m/s			
-16.22±451.87	71.91	0.0358	ids=25.8,iqs=25.8,idr=24.1,iqr=24.2
-3.55±11.63	1.85	0.2920	ids=1.9,iqs=44.8,wr=3,idr=2.1,iqr=48
-5.83	0	1	ids=47.2,iqs=0.9,idr=50.6,iqr=1.1
-0.75	0	1	ids=0.1,iqs=0.6,beta=98.4,idr=0.1,iqr=0.6

Table 6: Small Signal Stability Analysis of FSIG for Scenario 1 at Different Wind Speed

Case 2 Weak Connection Short Circuit Level 25 MVA			
Eigenvalues	**Frequency of Oscillation (in Hz)**	**Damping Ratio**	**Most influential state in the control of the Mode with their participation factor (in percentage)**
Wind Speed 7 m/s			
-25.04±528.78	84.15	0.0473	ids=26,iqs=26,idr=24,iqr=24
-4.33±32.96	5.24	0.1304	ids=23.4,iqs=24.4,wr=0.1,idr=25.4,iqr=26.5
-2.16	0	1	ids=18.5,iqs=4.8,wr=49.3,beta=1.8,idr=20.2,iqr=5.1
-0.86	0	1	ids=1.1,iqs=0.4,wr=3.2,beta=93.5,idr=1.2,iqr=0.4
Wind Speed 9 m/s			
-24.80±528.84	84.16	0.0468	ids=26,iqs=26,idr=24,iqr=24
-2.97±11.05	1.75	0.2596	ids=1,iqs=45.1,wr=3.7,idr=1.1,iqr=48.9
-5.31	0	1	ids=47.65,iqs=0.3,idr=51.6,iqr=0.4
-1.18	0	1	beta=99.9
Wind Speed 11 m/s			
-24.80±528.83	84.16	0.0468	ids=25.8,iqs=25.8,idr=24.1,iqr=24.2
-3.18±10.60	1.68	0.2879	ids=2.8,iqs=43.4,wr=3.4,idr=3.1,iqr=47
-4.81	0	1	ids=46.8,iqs=1,wr=0.1,idr=50.7,iqr=1.2
-0.75	0	1	ids=0.2,iqs=0.6,beta=98.1,idr=0.2,iqr=0.7

Table 7: Small Signal Stability Analysis of FSIG for Scenario 2 at Different Wind Speed

Case 1 Strong Connection Short Circuit Level 60 MVA			
Eigenvalues	**Frequency of Oscillation (in Hz)**	**Damping Ratio**	**Most influential state in the control of the Mode with their participation factor (in percentage)**
Wind Speed 7 m/s			
-16.26±452.3	71.99	0.0359	ids=25.8,iqs=25.9,idr=24,iqr=24.2
-2.47±67.81	10.79	0.0365	ids=0.8,iqs=36.9,wr=11.1,idr=0.8,iqr=39.5,wt=1, θtw=9.6
-6.38	----	1.0000	ids=48.2,idr=51.6
-2.58±10.73	1.71	0.2335	ids=0.2,iqs=45.6,wr=0.4,idr=0.3,iqr=48.8,wt=3.6,θtw=0.8
Wind Speed 9 m/s			
-16.25±452.2	71.98	0.0359	ids=25.8,iqs=25.9,idr=24,iqr=24.2
-2.49±67.41	10.73	0.0369	ids=1.4,iqs=36,wr=11.3,idr=1.41,iqr=38.6,wt=1.1,θtw=10
-5.83	----	1.0000	ids=47.3,iqs=0.9,idr=50.6,iqr=1
-2.84±10.50	1.67	0.2611	ids=2.3,iqs=43.7,wr=0.3,idr=2.5,iqr=46.8,wt=3.3,θtw=0.7
Wind Speed 10 m/s			
-16.25±452.2	71.98	0.0359	ids=25.8,iqs=25.9,idr=24,iqr=24.2
-2.49±67.38	10.72	0.0370	ids=1.4,iqs=36,wr=11.3,idr=1.41,iqr=38.6,wt=1.1,θtw=10
-5.78	----	1.0000	ids=47.2,iqs=1,idr=50.5,iqr=1
-2.87±10.48	1.67	0.2637	ids=2.5,iqs=43.5,wr=0.3,idr=2.7,iqr=46.7,wt=3.3,θtw=0.7

Table 8: Small Signal Stability Analysis of FSIG for Scenario 2 at Different Wind Speed

Case 2 Weak Connection Short Circuit Level 25 MVA			
Eigenvalues	**Frequency of Oscillation (in Hz)**	**Damping Ratio**	**Most influential state in the control of the Mode with their participation factor (in percentage)**
Wind Speed 7m/s			
-24.83±529.3	84.24	0.0469	ids=25.9,iqs=26,idr=24,iqr=24
-2.32±66.7	10.61	0.0347	ids=0.8,iqs=33.9,wr=13.7,idr=0.8,iqr=36.7,wt=1.4,θtw=12.4
-5.49	----	1.0000	ids=47.9,idr=51.9
-2.31±10.0	1.60	0.2242	ids=0.4,iqs=45,wr=0.4,idr=0.4,iqr=48.7,wt=4,θtw=0.8
Wind Speed 9m/s			
-24.82±529.3	84.24	0.0468	ids=25.9,iqs=26,idr=24,iqr=24
-2.34±66.2	10.54	0.0353	ids=1.2,iqs=32.8,wr=14.2,idr=1.2,iqr=35.5,wt=1.5,θtw=13.1
-4.80	----	1.0000	ids=46.8,iqs=1,idr=50.7,iqr=1.2
-2.65±9.7	1.55	0.2625	ids=3.2,iqs=42.4,wr=0.4,idr=3.5,iqr=46,wt=3.6,θtw=0.7

Wind Speed 10 m/s			
-24.82±529.3	84.23	0.0468	ids=25.9,iqs=26,idr=24,iqr=24
-2.34±66.2	10.53	0.0353	ids=1.2,iqs=32.7,wr=14.3,idr=1.2,iqr=35.5,wt=1.5,θtw=13.2
-4.73	----	1.0000	ids=46.7,iqs=1.1,idr=50.6,iqr=1.3
-2.68±9.707	1.54	0.2662	ids=3.5,iqs=42.1,wr=0.4,idr=3.8,iqr=45.7,wt=3.6,θtw=0.7

Table 9: Small Signal Stability Analysis of FSIG for Scenario 3 at Different Wind Speed

Case 1 Strong Connection Short Circuit Level 60 MVA			
Eigenvalues	**Frequency of Oscillation (in Hz)**	**Damping Ratio**	**Most influential state in the control of the Mode with their participation factor (in percentage)**
Wind Speed 7 m/s			
-16.27±452.2	71.98	0.0359	ids=25.8,iqs=25.8,idr=24.1,iqr=24.1
-2.55±69.7	11.10	0.0366	ids=24.5,iqs=14.7,wr=9.8,idr=26.3,iqr=15.7,wt=0.8,θtw=7.9
-2.44±11.9	1.89	0.2016	ids=28.6,iqs=17,wr=0.3,idr=30.7,iqr=18.1,wt=4,θtw=1.1
-6.49	----	1.0000	ids=18.2,iqs=30,idr=19.4,iqr=32.2,wt=4,θtw=0.8
-1.18	----	1.0000	beta=99.9
Wind Speed 9 m/s			
-16.75±453.2	72.13	0.0369	ids=25.7,iqs=26,idr=23.9,iqr=24.2
-2.03±89.2	14.19	0.0228	ids=15.9,iqs=30.8,wr=2,idr=17.1,iqr=33.1,θtw=0.9
-5.05±44.0	7.00	0.1142	ids=30,iqs=15.7,wr=1,idr=32.4,iqr=16.9,wt=0.8,θtw=3
-1.26	----	1.0000	ids=30.6,iqs=1.2,wr=4.3,beta=3,idr=33.2,iqr=0.3,wt=5.8
-0.39	----	1.0000	ids=6.7,iqs=0.3,wr=0.95,beta=78.4,idr=7.3,iqr=0.3wt=5.8
Wind Speed 11m/s			
-16.25±452.3	71.98	0.0359	ids=25.8,iqs=25.8,idr=24.1,iqr=24.1
-2.47±67.4	10.73	0.0366	ids=1.4,iqs=36,wr=11.3,idr=1.4,iqr=38.6,wt=1.1,θtw=9.9
-2.86±10.5	1.67	0.2622	ids=2.2,iqs=43.8,wr=0.3,idr=2.4,iqr=46.9,wt=3.8,θtw=0.7
-5.84	----	1.0000	ids=47.3,iqs=0.9,idr=50.6,iqr=1
-0.75	----	1.0000	ids=0.1,iqs=0.6,beta=98.4,idr=0.1,iqr=0.6

Table 10: Small Signal Stability Analysis of FSIG for Scenario 3 at Different Wind Speed

Case 2 Weak Connection Short Circuit Level 25 MVA			
Eigenvalues	**Frequency of Oscillation (in Hz)**	**Damping Ratio**	**Most influential state in the control of the Mode with their participation factor (in percentage)**
Wind Speed 7 m/s			
-25.27±529.0	84.20	0.0477	ids=26.1,iqs=26,idr=23.9,iqr=23.8
-2.06±71.8	11.43	0.0287	ids=21.5,iqs=24.1,wr=2.3,idr=23.5,iqr=26.4,wt=0.1,θtw=1.7
-8.27±50.4	8.03	0.1618	ids=23.8,iqs=21.9,wr=1.3,idr=26,iqr=23.8,wt=0.4,θtw=2.4
-1.47	----	1.0000	ids=9.1,wr=11.2,beta=2,idr=10,iqr=0.1,wt=67,θtw=0.2
-0.69	----	1.0000	ids=0.2,wr=0.3,beta=97,idr=0.3,wt=2
Wind Speed 9 m/s			
-24.83±529.4	84.25	0.0468	ids=25.9,iqs=26,idr=23.9,iqr=24
-2.28±66.7	10.62	0.0342	ids=1.5,iqs=33.4,wr=13.5,idr=1.5,iqr=36.2,wt=1.4,θtw=12.2
-2.44±10.1	1.60	0.2352	ids=1.1,iqs=44.3,wr=0.4,idr=1.2,iqr=48,wt=4,θtw=0.8
-5.31	----	1.0000	ids=47.7,iqs=0.2,idr=51.6,iqr=0.3
-1.19	----	1.0000	beta=99.9
Wind Speed 11 m/s			
-24.82±529.3	84.24	0.0468	ids=25.9,iqs=26,idr=23.9,iqr=24
-2.31±66.2	10.54	0.0349	ids=1.2,iqs=32.8,wr=14.2,idr=1.2,iqr=35.6,wt=1.5,θtw=13.1
-2.66±9.7	1.55	0.2635	ids=3.1,iqs=42.5,wr=0.4,idr=3.4,iqr=46,wt=3.65,θtw=0.7
-4.82	----	1.0000	ids=46.9,iqs=1,idr=50.7,iqr=1.1,
-0.76	----	1.0000	ids=0.2,iqs=0.6,beta=98.1,idr=0.2,iqr=0.7

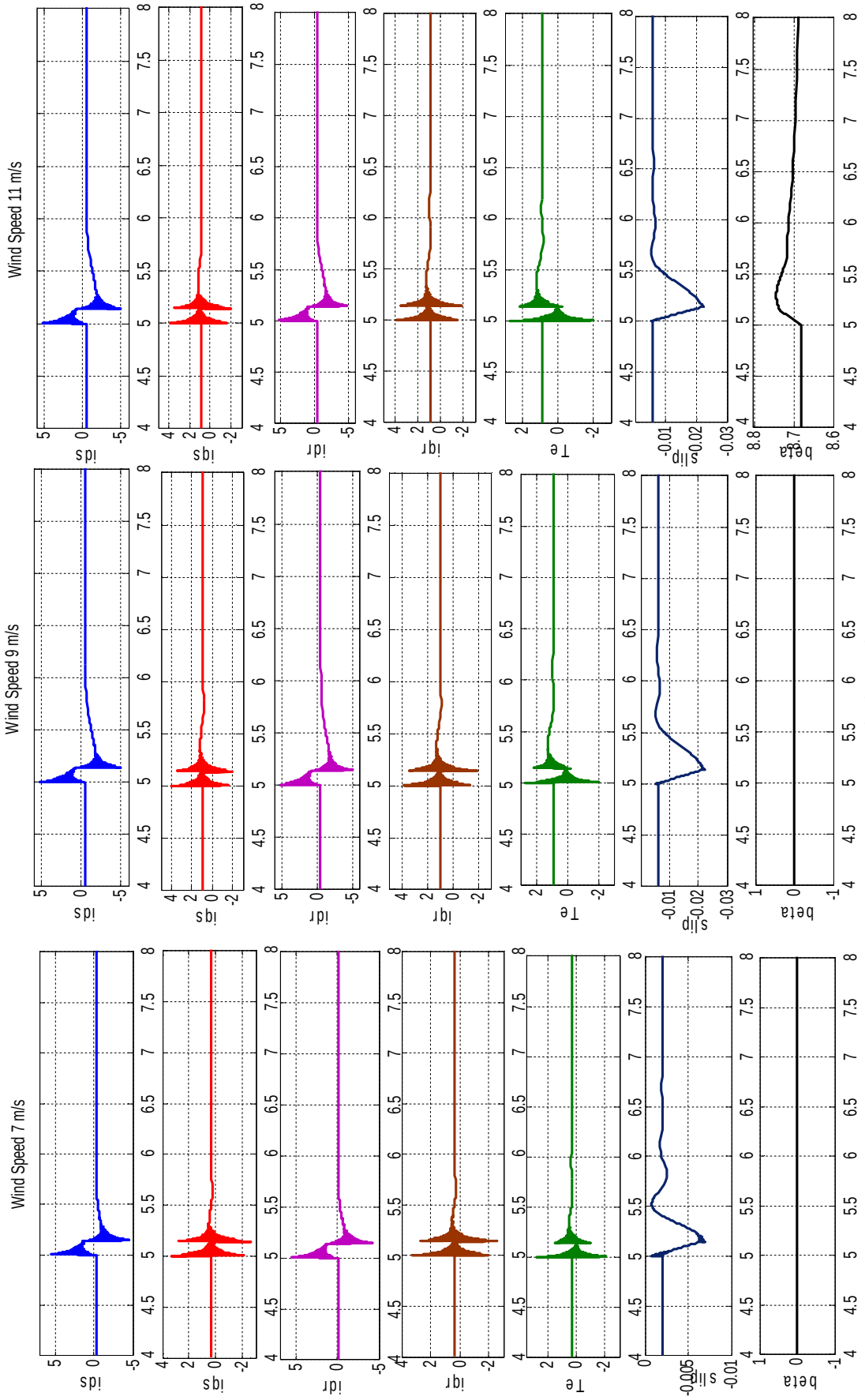

Fig.2. FSIG performance at different wind speed during three phase fault for scenario 1 (case 2 Weak Connection)

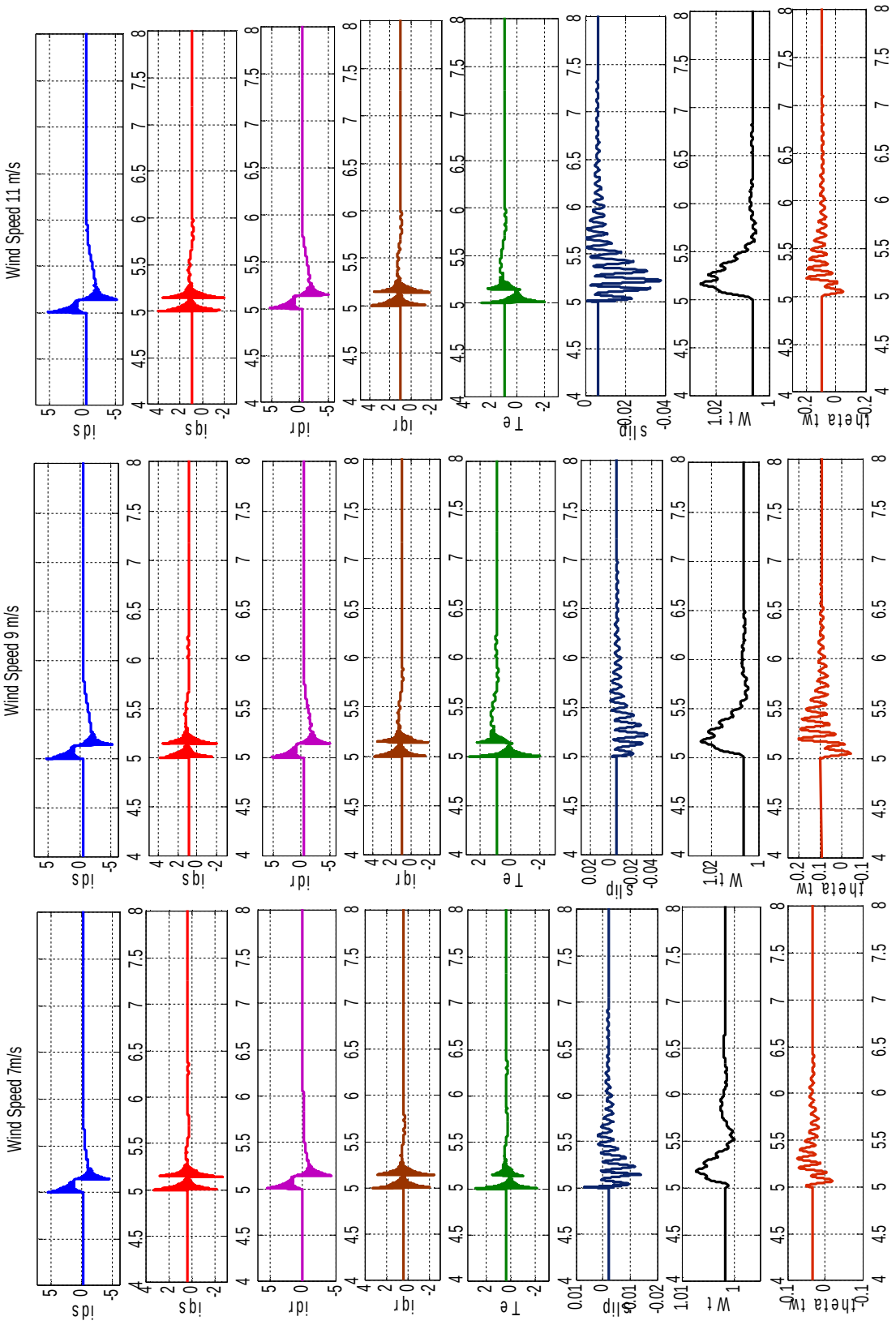

Fig.3. FSIG performance at different wind speed during three phase fault for scenario 2 (case 2 Weak Connection)

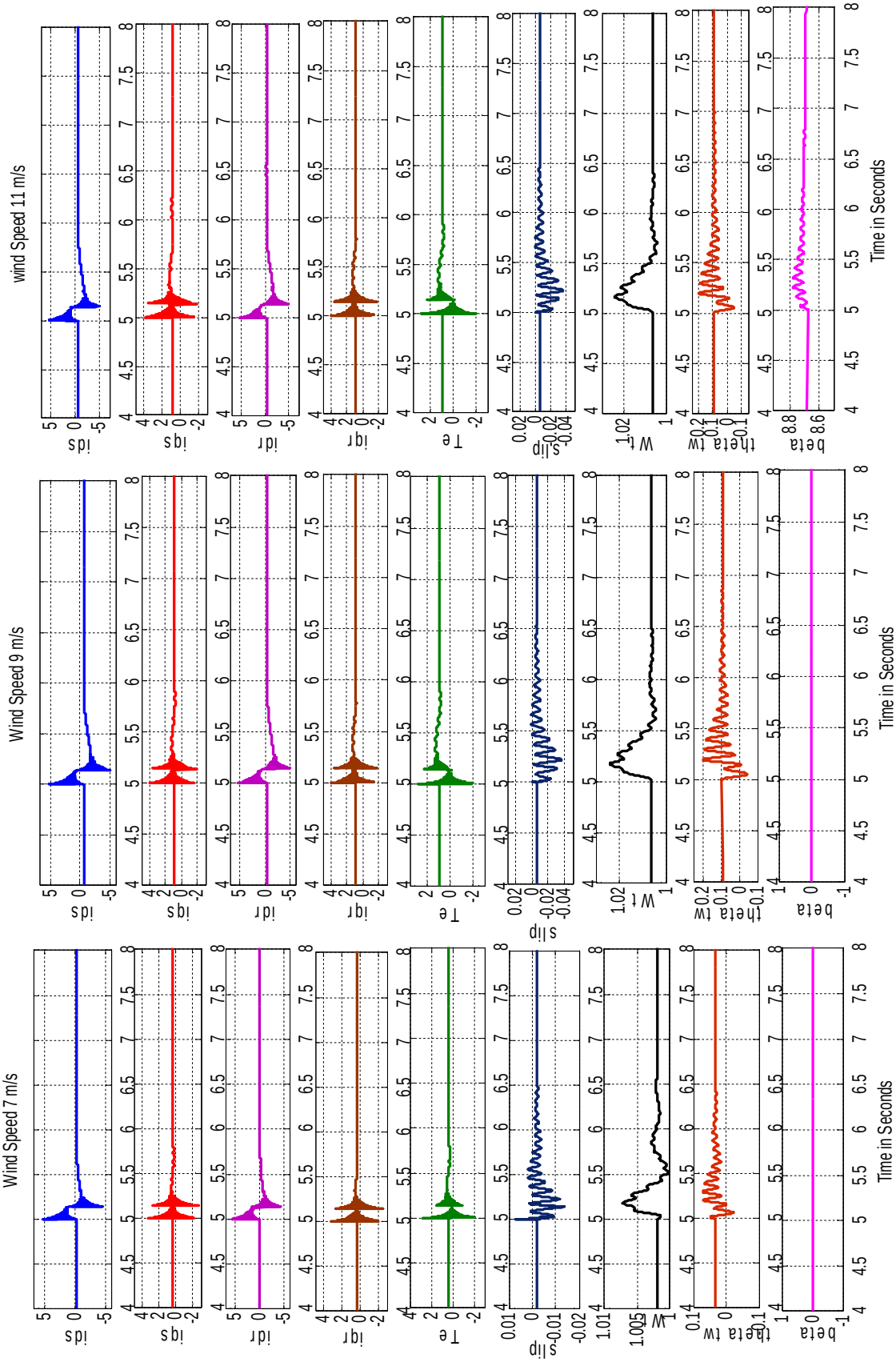

Fig.4. FSIG performance at different wind speed during three phase fault for scenario 3 (case 2 Weak Connection)

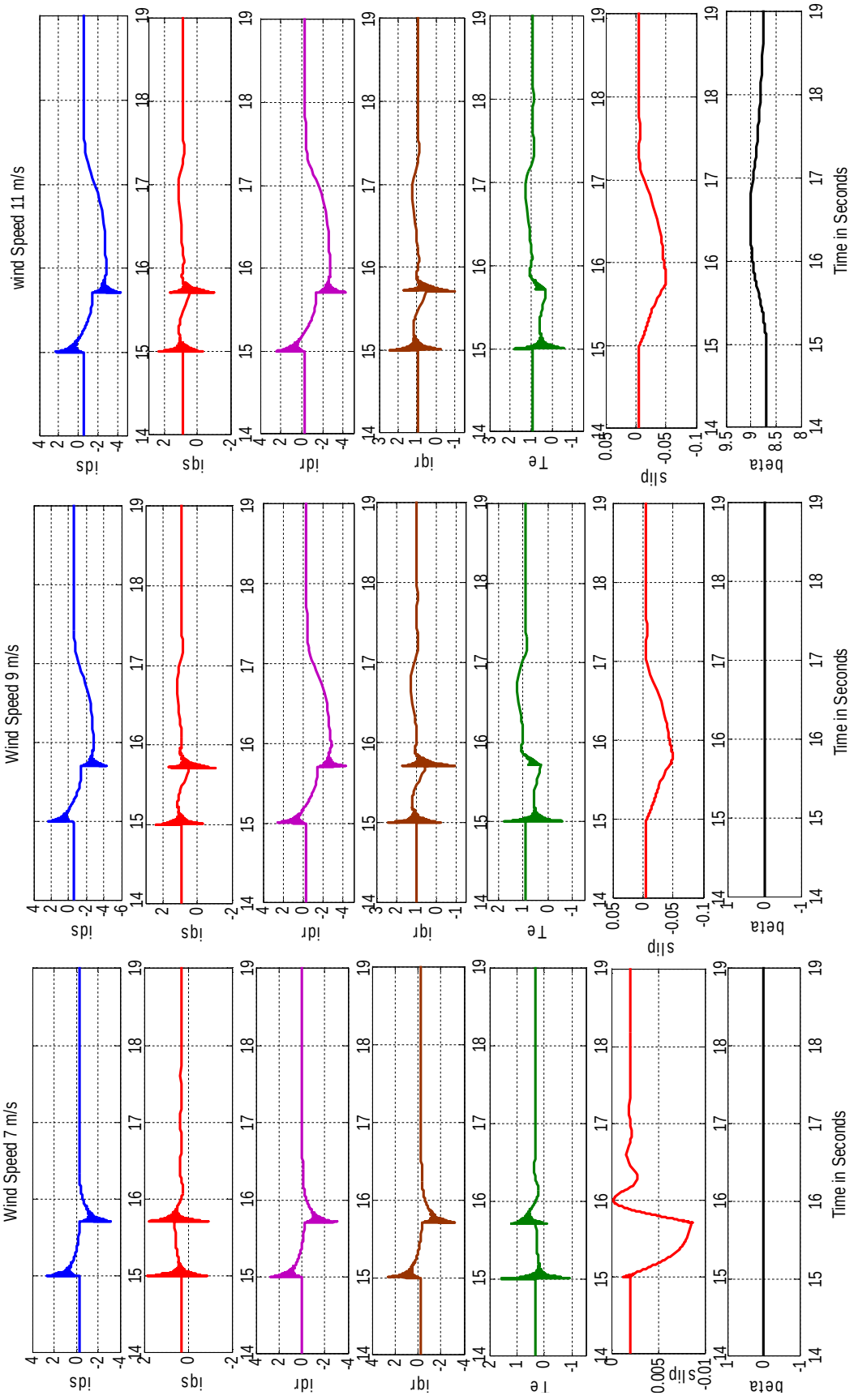

Fig.6. FSIG response 50% voltage sag at different wind speed for scenario 1 (case 2 Weak Connection)

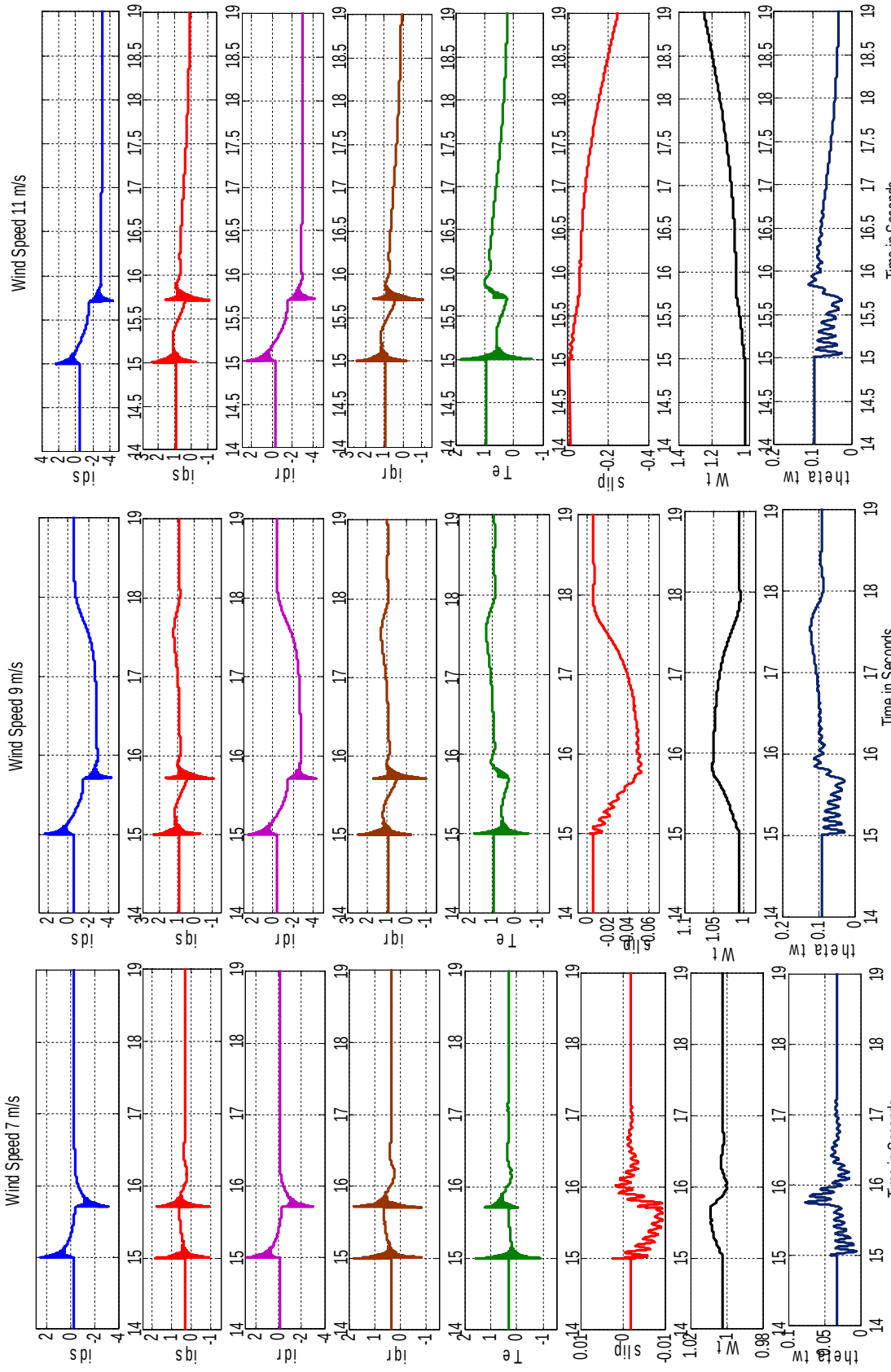

Fig.7. FSIG response 50% voltage sag at different wind speed for scenario 2 (case 2 Weak Connection)

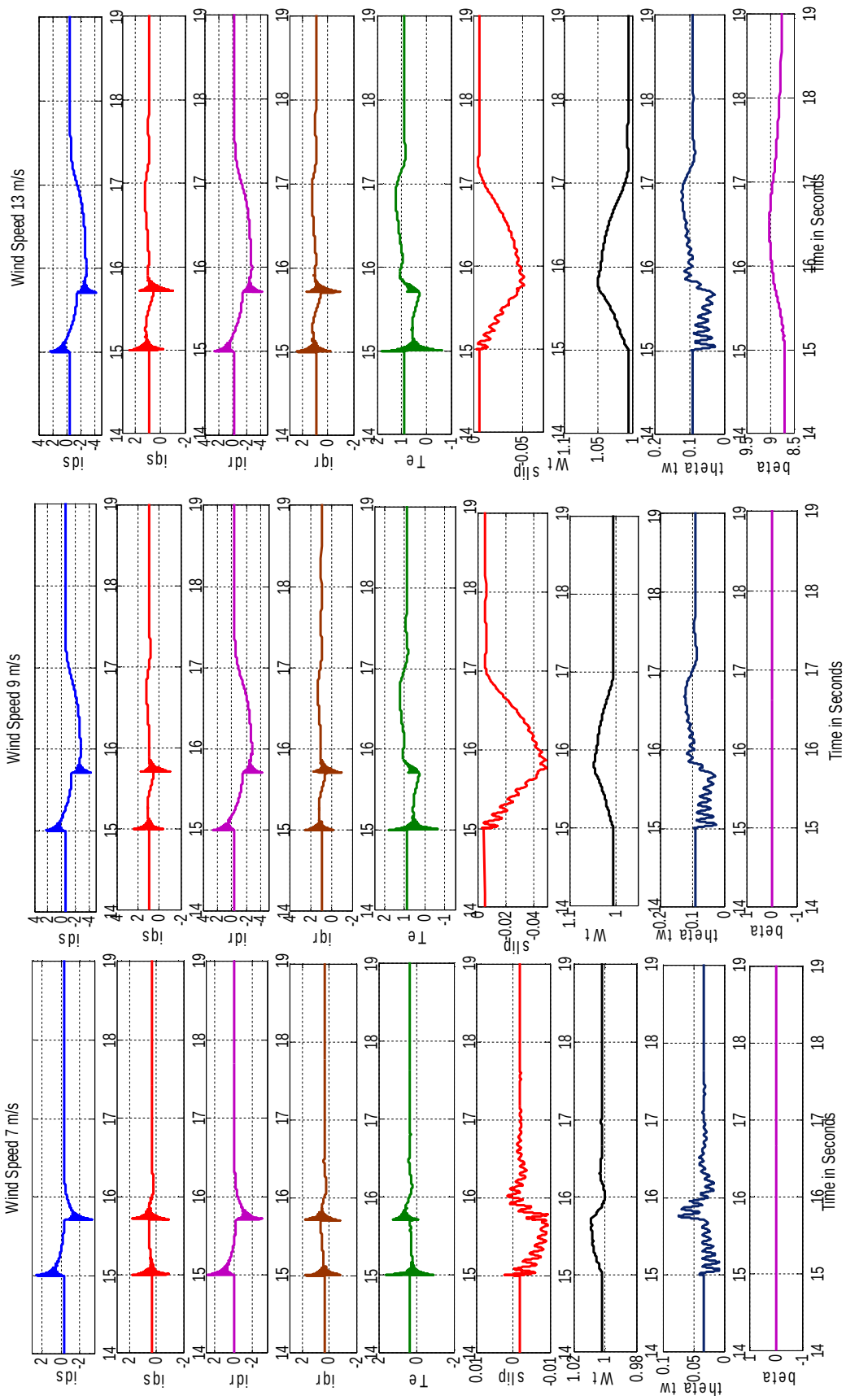

Fig.8. FSIG response 50% voltage sag at different wind speed for scenario 3 (case 2 Weak Connection)

The effects of varying wind speeds have been investigated for all three scenarios by observing the behaviour of different modes. It has been observed from the Tables 5-10, the mode $\lambda_{1,2}$ associated with stator dynamics remains unaffected while varying the wind speeds for all scenario. In scenario 1, the frequency of oscillation for mode $\lambda_{3,4}$ increases for the variation of wind speed from low to base wind speed. However, for base to high wind speed variations, the frequency of oscillation decreases. For scenario 2 and 3, this mode becomes non oscillating and hence exhibits the maximum damping. For scenario 3, the frequency of oscillations for low frequency oscillating mode decreases significantly for low to base wind speed whereas slight variation is observed for base to higher wind speed. Increased in the damping ratio is noticeable with the increase in wind speed. For the very high wind speed, the variation in frequency of oscillation for this mode remains unaltered due to activation of power limitation mode by pitch controllers.

4.3 Transient Response of FSIG

The transient performance of FSIG connected to infinite bus has been analyzed for three phase balanced fault applied at the terminal of infinite bus. The fault is applied at 5 seconds which persists for 140 milliseconds and the after that the normal operation is restored. The transient responses of different state variables, electromagnetic torque and slip for all three scenarios are depicted in Figs. 2-4 considering the weak connection of the network (VA_{SC} =25 MVA) with 7 m/s, 9 m/s and 11 m/s wind speeds. It is clearly observed from the Figs 2-4 that all the state variables are settled to the initial operating point before the application of the fault. The transient responses of electromagnetic torque and slip are also settled corresponding to wind speeds. These initial values of state variables, electromagnetic torque and slip are confirmed with the initialized values listed in Tables 2-4 for different scenarios. The occurrence of the fault creates large variations in transient responses of all the considered parameters.

The FSIG is able to carry the fault current magnitude up to 5 p.u. for a short duration and more sustained over current up to 2 p.u. The systems regain its original operating points after the removal of the fault and all the state variable are restored back. For the wind speed above the 9 m/s, the generated power may cross the rated power of the FSIG. Hence the action of the pitch angle controller needs to be activated to limit the power generation to a rated value. For scenario 1 and 3, the action of pitch angle controller can be observed from the Fig. 2 and 4. The action of pitch angle is also affected by the occurrence of fault but finally it is settled to the original operating point.

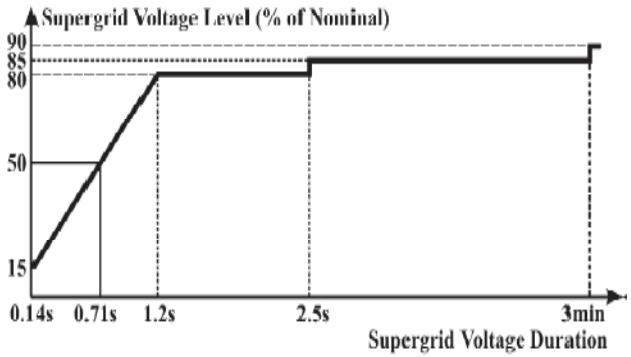

Fig.5 Fault ride-through capability demanded by the UK TSO [19].

The fault ride-through requirements specified in Grid Codes normally require the turbines to operate at reduced voltage for a few hundreds of ms to several seconds. The requirement specified by the TSO of UK is shown in Fig.5.where it can be seen that wind turbines should ride through a 50% fault for 710ms. This condition is investigated for all three scenarios under consideration and is shown in Figs. 6-8. It can be concluded that FSIG satisfy the grid code requirements.

5 Conclusion

Mathematical modelling of fixed speed induction generator connected to infinite bus for analysing small signal stability have been presented with the state space approach. The complete model of FSIG with considerations of one mass and two mass drive train models are presented which changes the order of the model and subsequently their effects on the modes of oscillations are studied. The stator dynamics remains unchanged irrespective of the model considered. The effect of two mass model has introduced an oscillating electromechanical modes whereas on the other hand its effect is responsible to completely damp the mode rotor dynamic. FSIG is capable of satisfying the Grid Code requirements of fault ride through under the three phase faults and voltage sag conditions.

References:

[1] [Online]http:www.windpowerindia.com

[2] Akhmatov V, Nielsen AH. Fixed-speed active-stall wind turbines in offshore applications. *European Trans Electrical Power* 2005;15:1–12.

[3] Trudnowski DJ, Gentile A, Khan JM, Petritz EM. Fixed-speed wind-generator and wind-park modelling for transient stability studies. *IEEE Trans Power Syst* 2004;19(4):1911–7.

[4] J.G.Slootweg, W.L.Kling, The impact of large scale wind power generation on power system oscillations, *Electric Power System Research*, vol.67, issue 1, pp.9-20, October 2003.

[5] Ackermann, T., 2005. *Wind power in power systems*. West Sussex, England: John Wiley & Sons, Ltd.

[6] Dong, Z.Y., et al., 2010. Wind power impact on system operations and planning. In: Proceedings of the *IEEE power and energy society general meeting*, 25–29 July 2010 Minneapolis, MN. Piscataway, NJ: IEEE, 1–5.

[7] S.Y. Kong , R.C. Bansal & Z.Y. Dong Comparative small-signal stability analyses of PMSG-, DFIG and SCIG-based wind farms, *International Journal of Ambient Energy* 2012, 33:2, 87-97.

[8] L. Holdsworth, X.G. Wu, J.B. Ekanayake, N. Jenkins,Comparison of fixed-speed and doubly-fed induction wind turbines during power system disturbances,*IEE Proc. Generation, Transm. Distrib.* Vol.150,no 3 pp 343–352, 2003.

[9] JanakaEkanayake and Nick Jenkins, Comparison of the Response of Doubly Fed and Fixed-Speed Induction Generator Wind Turbines to Changes in Network Frequency, *IEEETrans.EnergyConver*, vol. 19,no. 4, pp 800-802 December 2004.

[10] Jian Zhang , Adam Dy´sko b, John O'Reilly and William E. Leithead, Modelling and performance of fixed-speed induction generatorsin power system oscillation stability studies, *Electric Power Systems Research* vol. 78 pp 1416–1424,2008.

[11] Mohsen Rahimi and MostafaParniani, Dynamic behavior and transient stability analysis of fixed speed wind turbines, *Renewable Energy* vol,34pp. 2613–2624,2009

[12] P. Ledesma, J. Usaola, and J. L. Rodriguez, Transient stability of a fixed speed wind farm, *Renewable Energy*, vol. 28, pp. 1341-1355, May 2003.

[13] M. G. Kanabar, C. V. Dobariya, and S. A. Khaparde, Rotor Speed Stability Analysis of Constant Speed Wind Turbine Generators, in *Proc. IEEE International Conference on Power Electronics, Drives and Energy Systems*, PEDES, Dec. 2006.

[14] Carlos E. Ugalde-Loo, Janaka B. Ekanayake and Nicholas Jenkins, State-Space Modeling of Wind Turbine Generators for Power System Studies,*IEEE Trans. Industry Applications*, vol. 49, no. 1, pp. 223-232, January/February 2013

[15] P. Kundur,*Power System Stability and Control*, The EPRI Power System Engineering Series." McGraw-Hill,Inc, New York, 1994.

[16] P. C. Krause, O.Wasynczuk, and S. D. Sudhoff, *Analysis of Electric Machinery and Drive Systems*, Second Edition, A John Wiley and Sons,Inc.Publicaton, 2002.

[17] MATLAB Help Tutorial, The Math Works, Inc. Version 7.8.0.347, 2009.

[18] O. Anaya-Lara, N. Jenkins, J. B. Ekanayake, P. Cartwright, and M. Hughes, *Wind Energy Generation. Modelling and Control*. Hoboken, NJ: Wiley, 2009.

[19] Grid Code—Extra High Voltage, Tennet TSO GmbH,2010. [Online].Available:http://www.tennettso.de/site/binaries/content/assets/transparency/publications/grid connection/tennetnar2010eng.pdf

Appendix I

FSIG parameters in [p.u.] otherwise specified
D_{sh} = 0.01, K_{sh} = 10, H_{tot} = 3.5, H_g = 0.5, H_t = 3, V_{w_base} = 9 m/s, lambda = 8.1, cp = 0.48, P_{nom} = 2 MVA, P_{mec} = 2 MVA, P_{nom1} = 2.2222 MVA, P_{elec_base} = 2.2222 MVA, $P_{\_wind\_base}$ = 1, c1 = 0.5176, c2 = 116, c3 = 0.4, c4 = 5, c5 = 21, c6 = 0.0068, pitch_rate = 2, pitch_max = 45, K_p = 5, K_i = 25, V_b = 690 V, S_b = 2 MVA, F_b = 50, W_b = 2*pi*F_b, X_{tr} = 0.05, R_s = 0.00488, X_{ls} = 0.09241, R_r = 0.00549, X_{lr} = 0.09955, X_m = 3.95279, X_{rm} = 0.02, W_s = 1, X_{ss} = X_{ls} + X_m, X_{rr}=X_{lr} + X_m, vds_{inf} = 0, vqs_{inf} = 1

Appendix II

Type of Connection	Weak	Strong
S_b	2 MVA	2 MVA
VAsc	25 MVA	60 MVA
X/R	10	10
Z_e	0.08	0.033333333
R_e	0.007960298	0.003316791
X_e	0.079602975	0.033167906
R_t	0.012840298	0.008196791
X_t	0.129602975	0.083167906
X_m	3.95279	3.95279
X_e/X_m	0.020138428	0.008391011

Appendix III

$$E\frac{d}{dt}x = Fx + u$$

$$E = \frac{1}{\omega_b}\begin{bmatrix} -X_{ss} & 0 & X_m & 0 & 0 \\ 0 & -X_{ss} & 0 & X_m & 0 \\ -X_m & 0 & X_{rr} & 0 & 0 \\ 0 & -X_m & 0 & X_{rr} & 0 \\ 0 & 0 & 0 & 0 & 2H\omega_b \end{bmatrix}$$

$$F = \begin{bmatrix} -R & \omega^* X_{ss} & 0 & -\omega^* X_m & 0 \\ -\omega^* X_{ss} & -R & \omega^* X_m & 0 & 0 \\ 0 & s^*\omega^* X_m & R & -s^*\omega^* X_{rr} & \frac{X_{rr}^* i_{q0} - X_m^* i_{q0}}{\omega_b} \\ -s^*\omega^* X_m & 0 & s^*\omega^* X_{rr} & R & \frac{X_m^* i_{d0} - X_{rr}^* i_{d0}}{\omega_b} \\ -X_m^* i_{q0} & X_m^* i_{d0} & X_m^* i_{q0} & -X_m^* i_{d0} & 0 \end{bmatrix}$$

$$\dot{x} = Ax + Bu$$

$$y = Cx + Du$$

System matrix A, $A = (E)^{-1}F$

Control matrix B, $B = (E)^{-1}$

Output matrix C, $C = \begin{bmatrix} 0 & 0 & 1 & 0 & 0 \\ 0 & 0 & 0 & 1 & 0 \end{bmatrix}$

Feed forward matrix D, $D = \begin{bmatrix} 0 & 0 & 0 & 0 & 0 \\ 0 & 0 & 0 & 0 & 0 \end{bmatrix}$

Appendix IV

The elements of system matrix are as follows:

$$A_{11} = \frac{\omega_b}{X_{rr}X_{ss} - X_m^2}\{-R_s X_{rr} - R_e X_{rr}\}$$

$$A_{12} = \frac{\omega_b}{X_{rr}X_{ss} - X_m^2}\{(-X_{rr}X_{ss} + s0X_m^2)\omega_s - X_T X_{rr}\}$$

$$A_{13} = \frac{\omega_b}{X_{rr}X_{ss} - X_m^2}\{-R_r X_m\}$$

$$A_{14} = \frac{\omega_b}{X_{rr}X_{ss} - X_m^2}\{(X_m X_{rr} - s0X_m X_{rr})\omega_s\}$$

$$A_{15} = \frac{\omega_b}{X_{rr}X_{ss} - X_m^2}\{(-X_m ids0 + X_{rr} idr0)X_m\}$$

$$A_{21} = \frac{\omega_b}{X_{rr}X_{ss} - X_m^2}\{(X_{rr}X_{ss} - s0X_m^2)\omega_s + X_T X_{rr}\}$$

$$A_{22} = \frac{\omega_b}{X_{rr}X_{ss} - X_m^2}\{-R_s X_{rr} - R_e X_{rr}\}$$

$$A_{23} = \frac{\omega_b}{X_{rr}X_{ss} - X_m^2}\{(-X_m X_{rr} + s0X_m X_{rr})\omega_s\}$$

$$A_{24} = \frac{\omega_b}{X_{rr}X_{ss} - X_m^2}\{-R_r X_m\}$$

$$A_{25} = \frac{\omega_b}{X_{rr}X_{ss} - X_m^2}\{(X_m iqs0 - X_{rr} iqr0)X_m\}$$

$$A_{31} = \frac{\omega_b}{X_{rr}X_{ss} - X_m^2}\{-R_s X_m - R_e X_m\}$$

$$A_{32} = \frac{\omega_b}{X_{rr}X_{ss} - X_m^2}\{(-X_m X_{ss} + s0X_m X_{ss})\omega_s - X_T X_m\}$$

$$A_{33} = \frac{\omega_b}{X_{rr}X_{ss} - X_m^2}\{-R_r X_{ss}\}$$

$$A_{34} = \frac{\omega_b}{X_{rr}X_{ss} - X_m^2}\{(X_m^2 - s0X_{ss}X_{rr})\omega_s\}$$

$$A_{35} = \frac{\omega_b}{X_{rr}X_{ss} - X_m^2}\{(-X_m ids0 + X_{rr} idr0)X_{ss}\}$$

$$A_{41} = \frac{\omega_b}{X_{rr}X_{ss} - X_m^2}\{(X_m X_{ss} - s0X_m X_{ss})\omega_s + X_T X_m\}$$

$$A_{42} = \frac{\omega_b}{X_{rr}X_{ss} - X_m^2}\{-R_s X_m - R_e X_m\}$$

$$A_{43} = \frac{\omega_b}{X_{rr}X_{ss} - X_m^2}\{(-X_m^2 + s0X_{ss}X_{rr})\omega_s\}$$

$$A_{44} = \frac{\omega_b}{X_{rr}X_{ss} - X_m^2}\{-R_r X_{ss}\}$$

$$A_{45} = \frac{\omega_b}{X_{rr}X_{ss} - X_m^2}\{(X_m iqs0 - X_{rr} iqr0)X_{ss}\}$$

$$A_{51} = \frac{-X_m idr0}{2H}$$

$$A_{52} = \frac{X_m iqr0}{2H}$$

$$A_{53} = \frac{X_m ids0}{2H}$$

$$A_{54} = \frac{-X_m iqs0}{2H}$$

$$A_{55} = 0$$